GGA+U calculations of correlated spin excitations in $LaCoO_3$

Karel Knížek,[1] Zdeněk Jirák,[1] Jiří Hejtmánek,[1] Pavel Novák,[1] and Wei Ku[2]
[1]*Institute of Physics ASCR, Cukrovarnická 10, 162 53 Prague 6, Czech Republic*
[2]*Physics Department, Brookhaven National Laboratory, Upton, New York 11973, USA*
(Received 2 July 2008; revised manuscript received 24 November 2008; published 22 January 2009)

A comprehensive generalized gradient approximation (GGA)+U calculation study of many various Co^{3+} spin configurations for the model structures of $LaCoO_3$ was performed. In addition to the nonmagnetic ground state based on the low-spin (LS) Co^{3+}, the calculations evidence a number of stationary states based on the combinations of LS, high-spin (HS), and intermediate-spin (IS) Co^{3+} species. The stability of individual spin states is strongly conditioned by the character of neighboring spin states. If the amount of excited magnetic Co^{3+} ions in the LS matrix is small, their state is always of the HS kind. With an increasing number of Co^{3+} in HS states, a preference for antiparallel orientation of their spins appears and, at the same time, strong HS-HS nearest-neighbor correlations are evidenced. When the HS population in the LS matrix approaches a theoretical limit 1:1, further excitation to the HS state is hindered and alternative configurations based on clustering of the IS states become energetically favorable. Finally, the uniform Co (IS) configuration with preference for parallel spin alignment is stabilized. The present calculations are thus in agreement with a two-step LS-LS/HS-IS scenario of the electronic transitions in $LnCoO_3$, consisting of a local excitation of HS in LS matrix, which is followed by reversal of the thermally populated HS/LS pairs into the IS states.

DOI: 10.1103/PhysRevB.79.014430 PACS number(s): 75.30.Wx, 71.15.Mb

I. INTRODUCTION

The perovskites $LnCoO_3$ (Ln=La,Y,rare earth) exhibit an insulating ground state based on the diamagnetic low-spin (LS) state of Co^{3+} (S=0). With increasing temperature, all the compounds undergo two magnetic transitions that are generally interpreted in terms of Co^{3+} thermal excitations to the magnetic intermediate-spin (IS, S=1) or high-spin (HS, S=2) states. For $LaCoO_3$ the first transition is centered at T_{magn}=70 K and a stable paramagnetic insulating phase with Curie-Weiss character of susceptibility and pronounced antiferromagnetic (AFM) interactions is established above 100 K. Another change in susceptibility associated with a conductivity transition of the insulator-metal type occurs above room temperature and is centered at $T_{I\text{-}M}$=535 K.[1,2] With decreasing Ln size in other $LnCoO_3$ cobaltites, both transitions shift to higher temperatures and approach each other. In particular for $YCoO_3$, they develop practically concurrently at T_{magn}=780 K and at $T_{I\text{-}M}$=800 K.[3]

Various statistical models have been applied to describe the first transition, differing in the assignment of the lowest-excited state (IS or HS) and treatment of the nearest-neighbor interactions.[3–8] The IS Co^{3+} excitations seem to be supported, e.g., by analysis of magnetic susceptibility of $LnCoO_3$ (Ln=La,Pr,Nd),[9] analysis of thermal expansion obtained for $LaCoO_3$ by powder neutron diffraction,[10,11] dilatometry on single crystal,[5] neutron scattering,[12] and by temperature-dependent infrared spectroscopy of $LnCoO_3$ (Ln=La,Pr,Nd), where an increase in the intensities ascribed to the IS state was observed.[13] On the other hand, an alternative possibility of HS Co^{3+} low-temperature excitations is preferred in view of some recent experiments on $LaCoO_3$, including electron-spin resonance (ESR),[14] inelastic neutron scattering,[15] and x-ray magnetic circular dichroism (XMCD).[16]

A complex statistical model describing the two magnetic transitions in $LnCoO_3$ should involve both the IS and HS excitations.[8,10] This means that all three Co^{3+} spin states should be close in energy, which is an unexpected situation in transition-metal oxides (not predicted by standard crystal-field theory), pointing to a subtle balance between the kinetic energy, crystal-field splitting Δ_{CF}, on-site Coulomb repulsion expressed by Hubbard parameter U, and the energy of charge transfer between a transition metal and oxygen $\Delta_{TM\text{-}O}$. These effects can be effectively treated by the electronic structure calculations within the local-density approximation, LDA+U. Previous calculations performed within a structure with only a single crystallographically independent Co site gave only two energetically close stationary states in $LaCoO_3$—the diamagnetic insulating ground state characterized by Co^{3+} ions in the LS state and the excited stationary state of metallic character based on paramagnetic IS Co^{3+} ions.[17] This was tentatively taken as strong support for the IS character of $LaCoO_3$ above 100 K (LS-IS scenario of the first transition). Nevertheless, when two different Co sites were allowed within the LDA+U [or generalized gradient approximation (GGA)+U] method, an excited stationary state of insulating character based on the ordered LS and HS Co^{3+} species emerges at even lower energy than the homogeneous phase based on IS Co^{3+}.[18] This state was predicted also by the unrestricted Hartree-Fock method[19] and effective Hamiltonian calculations.[7,20,21] Its existence is an argument for opposing the LS-HS scenario of the low-temperature transition in $LaCoO_3$ and points to a certain tendency in cobaltites to diversify local Co^{3+} states, in which correlations and real electronic exchange play a decisive role. The early idea of dynamic LS+HS pairs[22] as constituents of the paramagnetic phase in $LaCoO_3$ is thus revived.

The aim of this work is to study by electron structure calculations various configurations of mixed LS, IS, and HS spin states, which may occur during the magnetic transitions as short-range-correlated structure in the $LnCoO_3$, and to determine the most probable of them. In our previous calcula-

tion within structures with two independent Co sites,[18] we have demonstrated the influence of correlations with neighboring ions on the spin state of Co^{3+}. The present calculations are performed for several model structures with parameters that correspond to various temperatures and *Ln* ions, all with four independent Co sites in the unit cell. Such choice of the model structure allows to investigate the correlations between neighboring Co^{3+} ions in much more detail and involves also effects of orbital ordering and CoO_6 octahedra distortion. The calculations confirm the HS Co^{3+} states as the first excitation level in $LnCoO_3$ and define conditions for stabilization of the homogenous IS phase. Finally, possible evolution of the spin states with temperature is proposed, in agreement with the LS-LS/HS-IS scenario recently postulated in Refs. 7 and 8.

II. METHOD OF CALCULATION

The calculations were made with the WIEN2k program.[23] This program is based on the density-functional theory (DFT) and uses the full-potential linearized augmented plane-wave (FP LAPW) method with the dual basis set. In the LAPW methods, the space is divided into atomic spheres and the interstitial region. The electron states are then classified as the core states that are fully contained in the atomic spheres and the valence states. The valence states are expanded using the basis functions; each of the basis functions has the form of the plane wave in the interstitial region, while it is an atomiclike function in the atomic spheres. To make possible treatment of two valence functions with the same orbital number (such as $3p$ and $4p$ functions of Co), so-called local orbitals are added to the basis functions.[24] In our calculations the electronic configuration of the core states corresponded to Ne ($3s^2$) for Co, to He for O, and to Kr ($4d^{10}$) for La atoms. The number n_k of the k points in the irreducible part of the Brillouin zone was 85 and the number n_b of the basis functions was $\approx$100 per atom in the unit cell. All calculations were spin polarized. For the exchange-correlation potential, the GGA form was adopted.[25] The radii of the atomic spheres were 2.30, 1.90, and 1.60 a.u. for La, Co, and O, respectively. To improve the description of Co $3d$ electrons we used the GGA+U method, which corresponds to the LDA+U method described in Refs. 26 and 27 with the GGA correlation potential instead of LDA. In the LDA+U-like methods, an orbitally dependent potential is introduced for the chosen set of electron states, which in our case are $3d$ states of Co. This additional potential has an atomic Hartree-Fock form but with screened Coulomb and exchange interaction parameters. The value U=2.7 eV was used, the same as in Ref. 18. The fully localized limit version of the GGA+U method was employed.

The self-consistent procedure that uses LDA or GGA often yields different solutions [e.g., ferromagnetic (FM) and antiferromagnetic (AFM)] for different initial spin densities. This feature is even more pronounced in the GGA+U (LDA+U) methods where often multiple solutions may be stabilized when the calculation is started with different occupations of the orbital states to which GGA+U is applied. Using this fact, the total energies of various spin configurations were obtained.

TABLE I. Co-O bond lengths, Co-O-Co bond angles, and cell volumes per formula unit (V/Z) of the model structures used for calculation. The last column indicates a phase, which approximately corresponds to the model structure.

Co-O (Å)	Co-O-Co (deg)	V/Z (Å^3)	Relevant structure
1.935	157	54.53	$PrCoO_3$ at 300 K
1.935	160	55.35	(La-Pr)CoO_3 at 5 K
1.935	163	56.07	$LaCoO_3$ at 300 K
1.960	160	57.53	
1.960	163	58.27	
1.960	166	58.90	$LaCoO_3$ at 1000 K

III. RESULTS

The motivation for this work was to investigate the influence of the correlations between Co neighbors on the spin state of Co^{3+} ions in dependence on the principal structural features of the Co environment, namely, the average Co-O bond lengths, Co-O-Co bond angles, and distortions of the breathing or axial types. Therefore we used model structures rather than the experimentally determined.

For the perovskite-type structures, the length of the Co^{3+}-O bond basically depends on the temperature and on the Co^{3+} spin state. The range of Co-O bond lengths was chosen according to experimentally determined values for $LaCoO_3$ within the temperature range up to 1000 K.[11] The Co-O-Co bond angle basically depends on the temperature and on the *Ln* ionic radius. The range of Co-O-Co bond angles was chosen to comprise experimentally determined values for $LaCoO_3$ up to 1000 K and room-temperature values for $PrCoO_3$ and $NdCoO_3$.[3] In total, the calculations were performed for six model structures: three with bond length of 1.935 Å and bond angles of 157°, 160°, and 163° and three structures with bond length of 1.960 Å and bond angles of 160°, 163°, and 166° (see Table I).

The crystal structure of $LnCoO_3$ is of the rhombohedral perovskite-type $R\bar{3}c$ containing 2 f.u. for $LaCoO_3$ and of the orthorhombic *Pbnm* type with 4 f.u. for the other $LnCoO_3$ with smaller rare-earth or yttrium cations. These two space groups differ in octahedral tilting along the z direction (see Fig. 1). To model different spin configurations, we considered a cell with symmetry lowered to $P\bar{1}$, in which the four Co sites are crystallographically independent. The use of the $P\bar{1}$ space group allows for both the *Pbnm* and $R\bar{3}c$ tilting patterns. Trial calculation for several spin configurations showed, however, that the influence of the different tilting patterns is negligible. Therefore, it was sufficient to focus on

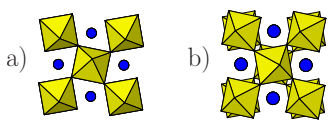

FIG. 1. (Color online) Comparison of the octahedra tilting in (a) *Pbnm* and (b) $R\bar{3}c$ space groups.

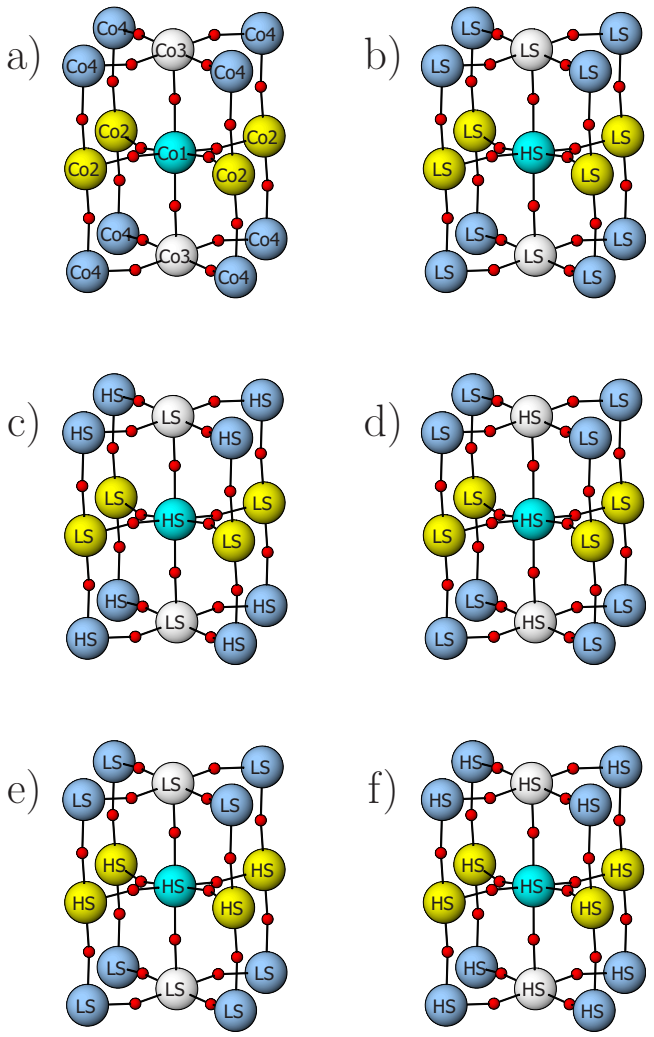

FIG. 2. (Color online) Examples of LS-HS configurations. Small red circles are oxygens; La atoms are omitted. (a) Labeling of four Co cations in $P\bar{1}$ space group. (b) Isolated magnetic Co in phase of HS/LS ratio 1:3. [(c)–(e)] Phases of HS/LS ratio 1:1 with isolated magnetic Co (six LS neighbors), chains of magnetic Co (four LS and two HS neighbors), and layers of magnetic Co (two LS and four HS neighbors). (f) The concentrated HS phase.

one of these structures, namely, on the *Pbnm* type. The labeling of Co cations, which is shown in Fig. 2(a), was chosen so that the nearest neighbors of Co1 in a distance of about 3.8 Å are four Co2 and two Co3 sites.

The energy of various spin configurations depends on both Co-O bond length and Co-O-Co bond angle. In this paper, we display the energy as a function of cell volume in order to show the dependence on a single variable. An example of the phase diagram, where the stability of LS and IS states is displayed in dependence on both bond length and angle, can be found in Ref. 28.

A. Diluted excited states

As the first step we tested possible spin states at the beginning of the first magnetic transition, when the population of excited states is low. For this purpose, calculations for a phase with ratio of magnetic to diamagnetic Co ions of 1:3 were attempted [see Fig. 2(b)]. The convergence could only be achieved for a cell with one HS and three LS states. The calculation for one IS and three LS states could not be stabilized and always converged to another configuration.

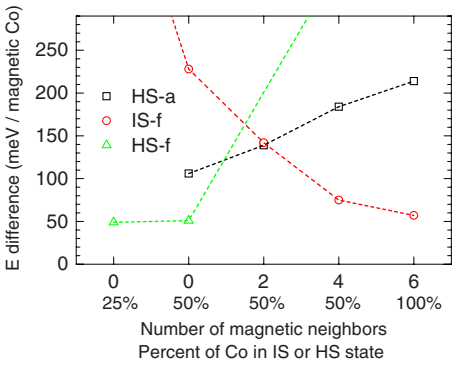

FIG. 3. (Color online) Relative energy in dependence on the number of magnetic neighbors and the ratio of magnetic ions. The corresponding configurations are successively displayed in Figs. 2(b)–2(f).

Additionally, we have tested also the case of isolated pair of excited IS or HS Co ions with parallel or opposite spin directions. For this purpose, we had to double the unit cell in the c direction. Among the four possible arrangements, the lowest energy was found for pair of HS states with antiferromagnetic alignment. The configurations with pair of Co in IS states converged to a stable solution, but they had significantly higher energy. The calculation for pair of Co in HS states with parallel spin alignment could not be stabilized. These calculations thus indicate that the HS state is the only allowed magnetic state at the first stages of the magnetic transition in $LnCoO_3$, where excited Co ions are isolated or in pairs with antiparallel spin orientation.

B. Effect of neighbors in the concentrated case

For the investigation of the possible spin states at the middle stage of the first magnetic transition, when the population of excited states is increased, it is important to know the preference of IS and HS Co ions to have as neighbors the magnetic (IS or HS) or nonmagnetic (LS) states. For this purpose, we have constructed cells with two Co in the LS state and two Co in the IS or HS state. For each magnetic state, we tested three configurations with various number of neighbors in the LS state, namely, with six LS neighbors [isolated magnetic Co; see Fig. 2(c)], four LS neighbors [chains of magnetic Co; see Fig. 2(d)], and two LS neighbors [layers of magnetic Co; see Fig. 2(e)]. Each configuration could be with parallel or opposite alignment of IS or HS spins.

The results expressed as energy per one magnetic Co relative to its LS ground state are displayed in Fig. 3. They are obtained for a cell with Co-O=1.935 Å and Co-O-Co =160°, which would correspond to average structures of $PrCoO_3$ and $LaCoO_3$ around 5 K (see Table I). In addition to the above-mentioned configurations (zero, two, and four magnetic neighbors; 50% of magnetic Co), we included for

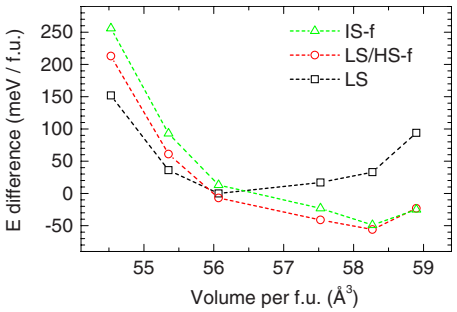

FIG. 4. (Color online) Relative energy for selected spin configurations in dependence on cell volume.

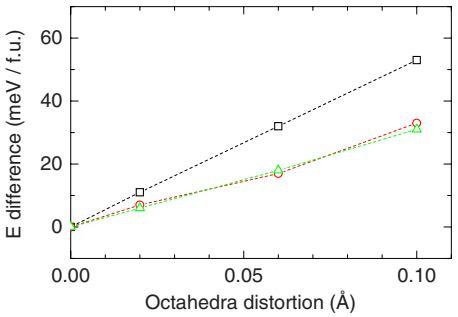

FIG. 5. (Color online) Relative energy dependence on octahedra distortion, i.e., the difference between long and short Co-O bonds. Types of distortions: (□) two longer and four shorter; (○) two shorter and four longer; and (△) two longer, two middle, and two shorter.

comparison the energy calculated for diluted excitation [zero magnetic neighbors and 25% of magnetic Co; see Fig. 2(b)] and for uniform spin configuration [six magnetic neighbors and 100% of magnetic Co; see Fig. 2(f)]. The ferromagnetic HS configurations with two and four Co(HS) neighbors were impossible to converge and their energy was estimated by interpolation.

The energies of configurations displayed in Fig. 3 evidence that for a small amount of excited Co ions the HS state is the only probable magnetic state. With increasing number of excited magnetic ions, when the probability of excitations of two neighbors is no longer negligible, an antiparallel orientation of HS spin states is preferred—as expected from the strong magnetic superexchange between neighboring high-spin configurations. The energy of isolated IS states is high but it decreases significantly with increasing number of neighbors in the IS state. Finally, for the concentrated case, the magnetic cations of the IS kind become preferable over the HS ones.

We have also tested various combinations of IS and HS states. However, we have not found any configuration with energy less than 100 meV above the ground state.

C. Dependence on the unit-cell volume

As a next step, we tested the dependence of relative stability of selected spin configurations on temperature. The increase in temperature was simulated by structural changes, namely, increase in volume induced by elongation of Co-O bonds and straightening of Co-O-Co bond angles. The considered structures are specified in Table I. The results of the calculation are summarized in Fig. 4.

The structures with smaller cell volume correspond to low temperature (shorter Co-O bond lengths and less linear Co-O-Co bond angles). Figure 4 shows that the most stable configuration in that case is the configuration with all four Co in the LS state, i.e., the diamagnetic ground state actually observed. This can be understood as the consequence of enhanced crystal-field splitting between the e_g and t_{2g} orbitals at smaller volume, which is sufficient to overcome the atomic Hund's coupling that favors higher spin configuration. For increasing cell volumes, which correspond to higher temperature (longer Co-O bond lengths and more linear Co-O-Co bond angles), the most stable configuration becomes the spin-mixed phase with two Co in the LS and two Co in the HS state [see Fig. 2(c)]. For the largest cell volume, there occurs a crossover to a homogeneous configuration with four Co in IS state ferromagnetically aligned. It is worth mentioning that the difference between the IS and LS/HS configurations remains quite small, whereas the destabilization of the LS configuration with increasing volume (temperature) is marked.

D. Jahn-Teller effects

Observation of the CoO_6 octahedra distortions is often claimed as evidence of the IS state as the electron configuration ($t_{2g}^5 e_g^1$) is expected to be Jahn-Teller active.[29–31] Therefore the investigation of various distortions of CoO_6 octahedra was undertaken within the concentrated IS spin configuration. Three types of the Jahn-Teller distortion were tested: (1) antiferrodistortive arrangement of tetragonally elongated CoO_6 octahedra, i.e., two longer and four shorter Co-O bonds; (2) antiferrodistortive arrangement of tetragonally shortened CoO_6 octahedra, i.e., two shorter and four longer Co-O bonds; and (3) orthorhombic distortion, i.e., two longer, two middle, and two shorter Co-O bonds. The dependence of energy per formula unit on the degree of distortion is displayed in Fig. 5. It is evident that any kind of axial distortion of CoO_6 octahedra destabilizes the structure.

Typically, stabilization of the structure due to Jahn-Teller-type distortion is common, e.g., in Mn^{3+} perovskites, where the e_g orbital electron-phonon coupling to the Jahn-Teller modes is enhanced by localization of electrons via local Coulomb interactions.[32–34] In particular, a recent first-principles study showed that the Coulomb interaction is essential to achieve the necessary degree of localization that supports large enough Jahn-Teller energy for orbital ordering. Without sufficient localization, the electron-phonon interaction was found insufficient to order the orbitals.[34] Therefore, the absence of favored orbital ordering in our results—even with open-shell e_g orbitals—suggests strongly that the degree of localization of the electrons in a structure of larger volume, where the IS configuration is found, is insufficient. A more detailed analysis will be given below after the large kinetic energy of the e_g orbital is illustrated clearly from the density of states (DOS).

E. Bond-length optimization

The ionic radius of Co^{3+} increases with the Co spin state, which is manifested by anomalies in lattice thermal expansion.[3,5,6,11] Therefore, further stabilization of the mixed spin configurations is achieved if the structure is relaxed to accommodate CoO_6 octahedra of different sizes. It was found in Ref. 18 that a breathing-type distortion is effective for stabilization of the ordered array 1:1 of HS and LS states corresponding to the configuration displayed in Fig. 2(c). This is understandable as the additional e_g electron in the HS state requires longer bond length to fit into the octahedron. The optimum difference between the Co(HS)-O and Co(LS)-O bond length was determined to be 0.06 Å. It should be noted that each Co in the HS state is surrounded by six Co in the LS and vice versa in this configuration and the CoO_6 octahedra, despite their different sizes, remain regular with six equal Co-O bond lengths.

In this work we focused on the diluted LS/HS configuration with one Co in the HS and three Co in the LS state [see Fig. 2(b)]. In this case the breathing-type expansion of Co site in the HS state makes the nearest-neighbor Co sites in the LS state not only smaller but also causes axial distortions of the respective CoO_6 octahedra. Although we have not tested particularly the energy of the LS state against the octahedra distortion, we may expect that the LS state is destabilized similarly as the IS state investigated in Sec. III D. In spite of such competing effect, we have found in model calculations that the 1:3 configuration is stabilized upon the expansion of the Co(HS) site and the minimum of energy is achieved for the difference between the Co(HS)-O and Co(LS)-O bond lengths of 0.06 Å, the same value as for the 1:1 configuration.

These results offer an alternative interpretation of the claimed observation of Jahn-Teller distortion in $LaCoO_3$. The observed distorted CoO_6 octahedra might actually be Co ions in the LS state distorted by the expanded neighbors in the HS state.

F. Density of states

The DOS of the LS configuration is displayed in Fig. 6. The character of the DOS is insulating with a gap of about 1 eV. The states just below E_F correspond to Co(t_{2g}) and O(p) states, whereas the states just above Fermi level are of Co(e_g) character.

Figure 7 shows the DOS of the diluted HS/LS configuration [see Fig. 2(b)]. The insulating character of the DOS is retained with a slightly decreased gap of about 0.7 eV. The states below Fermi level are mostly contributed by t_{2g} bands of Co in the LS state and O(p) bands. A sharp peak above Fermi level belongs to the Co-HS(t_{2g}) band. It means that the gap is of a charge-transfer character between Co(HS) and Co(LS) bands including hybridized O(p) orbitals. The total magnetic moment per unit cell is exactly $4\mu_B$. The integer value of magnetic moments is to be expected for a system with an energy gap at least in one of the spin channels (see Ref. 28). The magnetic moments localized on different sites are $2.9\mu_B$ for the central Co1(HS) ion, $0.2\mu_B$ for its nearest Co2(LS) and Co3(LS) neighbors, and $\sim 0\mu_B$ for next-nearest Co4(LS) neighbors [see Figs. 2(a) and 2(b) for an explanation of the Co labeling]. Due to hybridization, the sum $2.9+2\times 0.2+0=3.3\mu_B$ differs from the total value. It is worth mentioning that the calculation for the isolated LS/HS configuration [see Fig. 2(c)] showed $2.9\mu_B$ for the Co(HS) ions and $0.3-0.4\mu_B$ for Co(LS) sites. In real many-body Hilbert space, this hybridization effect would correspond to a correlated two-site wave function of the form $0.9|\mathrm{HS},\mathrm{LS}\rangle + 0.1|\mathrm{LS},\mathrm{HS}\rangle$.

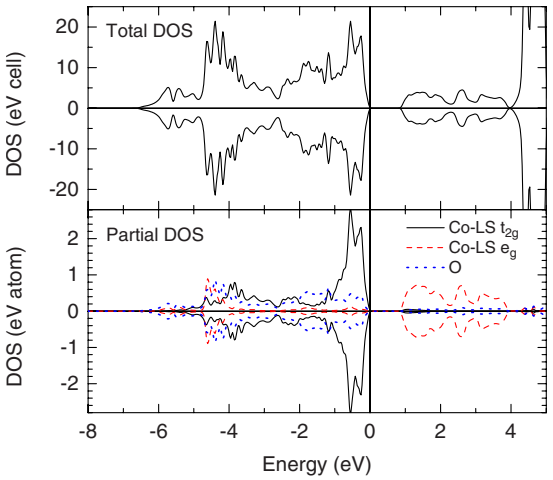

FIG. 6. (Color online) Density of states for LS configuration. Upper: total DOS; lower: projected DOS of Co e_g, Co t_{2g}, and O.

The DOS of the IS configuration is displayed in Fig. 8. The DOS has half-metallic character with conduction in the majority-spin channel only. The states on E_F are Co(e_g) for

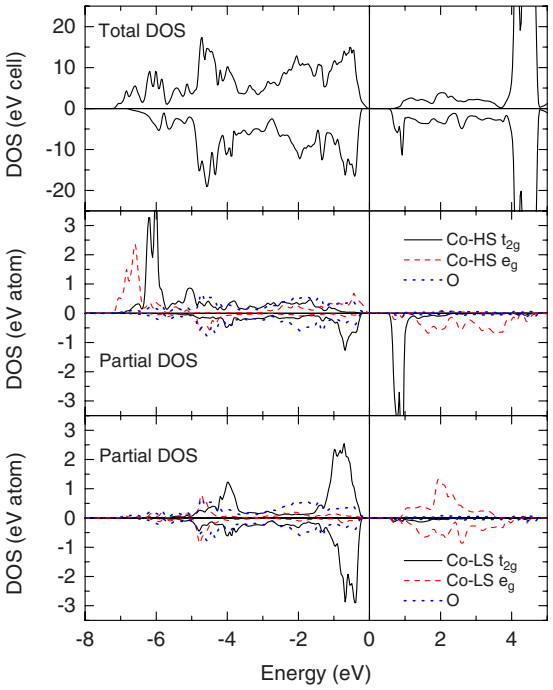

FIG. 7. (Color online) Density of states for HS/LS 1:3 configuration [see Fig. 2(b)]. Upper: total DOS; middle: projected DOS of HS Co e_g, Co t_{2g}, and O; and lower: projected DOS of LS Co e_g, Co t_{2g}, and O.

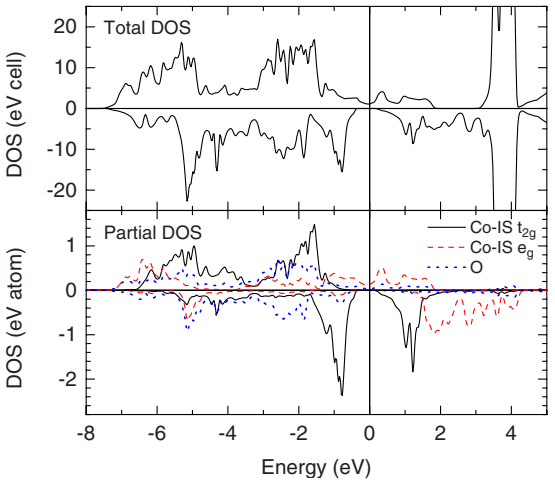

FIG. 8. (Color online) Density of states for IS configuration. Upper: total DOS; lower: projected DOS of Co e_g, Co t_{2g}, and O.

spin up and about 0.4 eV below E_F are Co(t_{2g}) for spin down. The Co states are strongly hybridized with the oxygen p states. The total magnetic moment per unit cell is $4\mu_B$. The magnetic moment on individual Co(IS) ions is $1.9\mu_B$ and differs from the ideal value $2\mu_B$ due to hybridization.

IV. DISCUSSION

The present calculations provide strong arguments that the paramagnetic phase in $LaCoO_3$ above 100 K is a result of gradual population of HS states in the LS matrix. The excitation of HS states is not a statistically independent event but is conditioned by the presence of the LS states at nearest sites. Nevertheless, a small amount of AFM-coupled Co(HS) pairs can exist. Since the interaction among the isolated Co(HS) ions is weak, the small number of the neighboring Co(HS) is responsible for the prevailing antiferromagnetic type of susceptibility in the solid. With increasing temperature, the phase tends to an ordered arrangement of HS and LS states in the 1:1 ratio. However, the entropy contribution, which is not included in our calculation, may destabilize this ordered configuration compared to randomly distributed Co(HS) in the Co(LS) matrix and thus prevents its formation. On the other hand, the isolated IS states should never exist in the LS matrix but larger IS clusters can be stabilized. The IS population thus tends to a formation of IS rich regions, which may exist within the LS/HS phase—either in the form of static phase separation or as part of the configurations of quantum fluctuation. The HS state is further stabilized if Co(HS) site is expanded (breathing-type distortion) at the expense of neighboring Co(LS) sites. On the other hand, the calculation for the concentrated IS phase shows that any kind of cooperative axial distortion of CoO_6 octahedra (Jahn-Teller effect) would destabilize the structure. We propose that the experimental observations of distorted CoO_6 octahedra actually reflect the Co^{3+} ions in the LS state distorted by the expanded neighbors in the HS state.

Our first-principles results can be summarized into a consistent microscopic picture containing competition between the crystal-field splitting, the local Hund's coupling, and the kinetic energy. At small volume, when the Co-O-Co bond angle is bent, the crystal field is dominant and leads to a LS configuration. As the volume increases, the crystal field decreases and Hund's coupling becomes relevant, leading to the formation of HS states where the e_g orbitals prefer longer Co-O bond length, even at the expense of the neighboring LS configuration. With further volume increase, the kinetic energy prevails with a straighter Co-O-Co bond angle. The e_g electrons become more itinerant and lose occupation due to rather large corresponding bandwidth, giving one additional charge to the t_{2g} orbital. Our results suggest that it might be more appropriate to consider the so-called IS configuration using an itinerant picture than a local picture commonly employed, at least in a clean sample. This itinerant nature of the IS configuration also provides a natural explanation for the lack of Jahn-Teller distortion in our results. Without sufficient degree of localization, electron-phonon coupling, such as the Jahn-Teller coupling, is insufficient to drive the orbital ordering, as recently shown by a first-principles study of the strongly orbital-ordered manganites.[34]

Note, however, like all the theoretical calculations with small system size, our small unit-cell calculation unavoidably maximizes the coherency and minimizes the fluctuation. Therefore, we expect that the local nature of the IS configuration in real materials might be slightly enhanced, as well as the effectiveness of the Jahn-Teller coupling. Similarly, the lack or freedom in the many-body Hilbert space of our DFT solution is expected to overestimate the degree of metallicity in our IS configuration. Nevertheless, given the good record of DFT in describing energy and spin density, we believe the trends derived from our calculations to be very close to the short-range-correlated structure in real materials.

Based on these findings we propose the following LS-LS/HS-IS scenario for the evolution of spin states with temperature. The ground state of $LaCoO_3$ is characterized by all Co^{3+} ions being in the LS state. The LS phase is diamagnetic and insulating with a gap of about 1 eV. The diamagnetic-paramagnetic transition is caused by gradual population of HS states with increasing temperature. The experimentally observed excitation energy at 150–200 K for $LaCoO_3$ (Refs. 3, 5, and 6) is responsible for a rapidly increasing population of HS states at $T_{\mathrm{magn}} \sim 70$ K. The slowing down in higher temperatures should be related to a gradual depletion of available sites for the HS excitation, requiring the LS states in their immediate neighborhood. With increasing number of Co^{3+} in HS states, when the probability of excitations of two neighbors is no longer negligible, an antiparallel orientation of HS spin states is preferred. The concentrated LS/HS phase is a paramagnetic insulator (gap ~ 0.5 eV). With further increase in temperature, the regions of the LS/HS phase are progressively reverted to the IS clusters. This process starts at about 350 K for $LaCoO_3$ and the energy of excitation to IS state is decreasing with increasing number in IS neighbors. Finally, at the second magnetic transition $T_{\mathrm{I\text{-}M}} \sim 500$ K connected with the insulator-metal transition, the clusters of IS states coagulate into domains of the homogeneous IS phase of metallic character, which is paramagnetic with the preference for parallel spin alignment. The spin-state transitions are thus a two-step process, in which the LS $\rightarrow$ HS and

LS/HS→IS excitations are practically separated in temperature for $LaCoO_3$; while for compounds with smaller rare-earth ions the HS and IS states are populated nearly simultaneously.

It should be noted that the excited HS and IS Co^{3+} are orbitally triply degenerate ionic species, which give rise to spin-orbit multiplets. The instructive diagram of electronic levels in dependence on the crystal-field splitting 10 Dq is presented in Fig. 2 of Ref. 16. The spin-orbit coupling in the HS Co^{3+} ions is discussed in more detail in Ref. 20. The excitation energy depends also on the temperature or pressure-induced changes in structural parameters, namely, of the Co-O bond length and Co-O-Co bond angle, which is confirmed experimentally by observation of pressure-induced spin transitions,[35,36] and is also in agreement with linear dependence of the critical temperatures on the *Ln* ionic radius and therefore on the Co-O-Co bond angle.[3,37]

Results of the present calculation are in agreement with a model proposed in our recent paper.[8] There we used an approximative model considering the Boltzmann statistics of LS/LS-LS/HS-IS/IS pairs to avoid the problem of strong HS-LS correlations and fitted magnetic susceptibility and thermal expansion of Co-O bonds for $LnCoO_3$ (Ln=La,Pr,Nd,Y) up to 1000 K. We assumed a Curie-Weiss type of paramagnetic susceptibility with significant antiferromagnetic contribution above the first magnetic transition and the second transition was explained as a population of IS states. According to this picture, the observed susceptibility step is an effect of change from local AFM coupling toward more itinerant FM ones, while the effective moments remained approximately the same.

V. CONCLUSIONS

The present GGA+U calculations evidence that two magnetic phases may exist in $LnCoO_3$ perovskites, in addition to the nonmagnetic LS ground state. The first one is a result of gradual population of HS states conditioned by the presence of the LS states at the nearest Co sites. Nevertheless, some Co(HS) pairs present are responsible for prevailing antiferromagnetic interactions. The mixed LS/HS phase tends to a short-range-ordered 1:1 arrangement, whose long-range formation is presumably prevented by the increased entropy. The second phase consists of large IS clusters, which may exist within the LS/HS phase and finally tend to a formation of uniform itinerant IS phases with ferromagnetic coupling. Thus the calculations are in agreement with a two-step LS-LS/HS-IS scenario of the electronic transitions in $LnCoO_3$.[7,8]

The HS state in the LS matrix is further stabilized if the Co(HS) site is expanded (breathing type) at the expense of neighboring Co(LS) sites. On the other hand, any kind of cooperative axial distortion of CoO_6 octahedra destabilizes the structure. We propose that the experimental observations of distorted CoO_6 octahedra actually reflect the Co^{3+} ions in the LS state distorted by the expanded neighbors in the HS state.

The magnetic susceptibility can be analyzed as excitations from the ground LS state to magnetic states with different excitation energy: HS with the lower and IS with the higher energy. However, the thermodynamic model is complex and must take into account: (1) dependence of the excitation energy of one Co site on the spin state of the neighboring Co sites; (2) varying ferro/antiferromagnetic interactions in dependence on the population of HS states (AFM) and IS states (FM) manifested in the temperature dependence of Weiss θ; (3) dependence of the excitation energies on the temperature or pressure-induced structural changes; (4) metallic character of the IS spin state, where a Pauli susceptibility contribution is possible; and (5) splitting of single excitation energy into multiplets due to the spin-orbit coupling, in particular for a small number of isolated HS states.

ACKNOWLEDGMENTS

This work was supported by the Grant Agency of the Czech Republic under Project No. 202/06/0051. Part of this work was supported by the Grant Agency of the ASCR under Project No. A100100611. The authors acknowledge support from project LUNA for help in performing the calculations. W.K. acknowledges support from the DOE under Grant No. DE-AC02-98CH10886 and DOE-CMSN.

[1] R. R. Heikes, R. C. Miller, and R. Mazelsky, Physica (Amsterdam) **30**, 1600 (1964).
[2] P. M. Raccah and J. B. Goodenough, Phys. Rev. **155**, 932 (1967).
[3] K. Knížek, Z. Jirák, J. Hejtmánek, M. Veverka, M. Maryško, G. Maris, and T. T. M. Palstra, Eur. Phys. J. B **47**, 213 (2005).
[4] M. Kurzyński, J. Phys. C **11**, 3179 (1978).
[5] C. Zobel, M. Kriener, D. Bruns, J. Baier, M. Grüninger, T. Lorenz, P. Reutler, and A. Revcolevschi, Phys. Rev. B **66**, 020402(R) (2002).
[6] J. Baier, S. Jodlauk, M. Kriener, A. Reichl, C. Zobel, H. Kierspel, A. Freimuth, and T. Lorenz, Phys. Rev. B **71**, 014443 (2005).
[7] T. Kyômen, Y. Asaka, and M. Itoh, Phys. Rev. B **71**, 024418 (2005).
[8] K. Knížek, Z. Jirák, J. Hejtmánek, P. Henry, and G. André, J. Appl. Phys. **103**, 07B703 (2008).
[9] J.-Q. Yan, J.-S. Zhou, and J. B. Goodenough, Phys. Rev. B **70**, 014402 (2004).
[10] K. Asai, A. Yoneda, O. Yokokura, J. M. Tranquada, G. Shirane, and K. Kohn, J. Phys. Soc. Jpn. **67**, 290 (1998).
[11] P. G. Radaelli and S.-W. Cheong, Phys. Rev. B **66**, 094408 (2002).
[12] K. Asai, O. Yokokura, N. Nishimori, H. Chou, J. M. Tranquada, G. Shirane, S. Higuchi, Y. Okajima, and K. Kohn, Phys. Rev. B **50**, 3025 (1994).
[13] L. Sudheendra, Md. Motin Seikh, A. R. Raju, and Chandrabhas Narayana, Chem. Phys. Lett. **340**, 275 (2001).

[14] S. Noguchi, S. Kawamata, K. Okuda, H. Nojiri, and M. Motokawa, Phys. Rev. B **66**, 094404 (2002).
[15] A. Podlesnyak, S. Streule, J. Mesot, M. Medarde, E. Pomjakushina, K. Conder, A. Tanaka, M. W. Haverkort, and D. I. Khomskii, Phys. Rev. Lett. **97**, 247208 (2006).
[16] M. W. Haverkort *et al.*, Phys. Rev. Lett. **97**, 176405 (2006).
[17] M. A. Korotin, S. Yu. Ezhov, I. V. Solovyev, V. I. Anisimov, D. I. Khomskii, and G. A. Sawatzky, Phys. Rev. B **54**, 5309 (1996).
[18] K. Knížek, Z. Jirák, J. Hejtmánek, and P. Novák, J. Phys.: Condens. Matter **18**, 3285 (2006).
[19] M. Zhuang, W. Zhang, and N. Ming, Phys. Rev. B **57**, 10705 (1998).
[20] Z. Ropka and R. J. Radwanski, Phys. Rev. B **67**, 172401 (2003).
[21] S. W. Biernacki, Phys. Rev. B **74**, 184420 (2006).
[22] M. A. Señarís-Rodríguez and J. B. Goodenough, J. Solid State Chem. **116**, 224 (1995).
[23] P. Blaha, K. Schwarz, G. K. H. Madsen, D. Kvasnicka, and J. Luitz, *WIEN2k: An Augmented Plane Wave+Local Orbitals Program for Calculating Crystal Properties* (Technische Universität, Wien, 2001).
[24] D. J. Singh and L. Nordström, *Plane Waves, Pseudopotentials, and the LAPW Method* (Springer, New York, 2005).
[25] J. P. Perdew, K. Burke, and M. Ernzerhof, Phys. Rev. Lett. **77**, 3865 (1996).
[26] V. I. Anisimov, I. V. Solovyev, M. A. Korotin, M. T. Czyzyk, and G. A. Sawatzky, Phys. Rev. B **48**, 16929 (1993).
[27] A. I. Liechtenstein, V. I. Anisimov, and J. Zaanen, Phys. Rev. B **52**, R5467 (1995).
[28] K. Knizek, P. Novak, and Z. Jirak, Phys. Rev. B **71**, 054420 (2005).
[29] D. Louca and J. L. Sarrao, Phys. Rev. Lett. **91**, 155501 (2003).
[30] A. Ishikawa, J. Nohara, and S. Sugai, Phys. Rev. Lett. **93**, 136401 (2004).
[31] S. K. Pandey, S. Khalid, N. P. Lalla, and A. V. Pimpale, J. Phys.: Condens. Matter **18**, 10617 (2006).
[32] V. I. Anisimov, I. S. Elfimov, M. A. Korotin, and K. Terakura, Phys. Rev. B **55**, 15494 (1997).
[33] J. E. Medvedeva, M. A. Korotin, V. I. Anisimov, and A. J. Freeman, Phys. Rev. B **65**, 172413 (2002).
[34] W.-G. Yin, D. Volja, and W. Ku, Phys. Rev. Lett. **96**, 116405 (2006).
[35] T. Vogt, J. A. Hriljac, N. C. Hyatt, and P. Woodward, Phys. Rev. B **67**, 140401(R) (2003).
[36] D. P. Kozlenko, N. O. Golosova, Z. Jirák, L. S. Dubrovinsky, B. N. Savenko, M. G. Tucker, Y. Le Godec, and V. P. Glazkov, Phys. Rev. B **75**, 064422 (2007).
[37] S. Yamaguchi, Y. Okimoto, and Y. Tokura, Phys. Rev. B **54**, R11022 (1996).